RSC Advances

PAPER

View Article Online
View Journal | View Issue

Cite this: *RSC Adv.*, 2025, **15**, 33264

Noscapine-loaded collagen-based silver nanoparticles: a potent nano-therapeutic approach for cancer treatment

Heerak Chugh,†[a] Nistha Mishra,†[ab] Shipra Chandra,[e] Jai Gopal Sharma[b] and Ramesh Chandra *[acd]

In this study, we investigated a method to develop multicomponent biodegradable nanoparticles for the delivery of noscapine to exploit its anti-proliferative, anti-cancer potential. The multicomponent nanoparticles were composed of a silver core stabilized with a collagen coating and loaded with noscapine (Ag-Col-Nos-NPs). Different concentrations of each component, molar ratios, reaction setup, and other variables were explored to optimize the final reaction. Ag-Col-Nos-NPs were then characterized for their physicochemical properties using UV-visible spectroscopy, Dynamic Light Scattering (DLS), Transmission Electron Microscopy (TEM), X-ray diffraction (XRD), Energy-Dispersive X-ray Spectroscopy (EDS) and, Fourier-Transform Infrared (FTIR). Evaluation of *in vitro* drug release and the cytotoxic potential of Ag-Col-Nos-NPs in an *in vitro* model of non-small cell lung cancer (H1299) displayed increased solubility and sustained release of noscapine with less deviation. In conclusion, our study observed Ag-Col-Nos-NPs as potential and stable carriers for the delivery of noscapine and other hydrophobic drugs to enable their therapeutic use.

Received 28th May 2025
Accepted 25th July 2025

DOI: 10.1039/d5ra03766b

rsc.li/rsc-advances

1. Introduction

Nanoparticles (NPs), defined as materials with sizes ranging between 1–100 nm have emerged as foundational building blocks in modern biomedical science, particularly in diagnosis, imaging and targeted therapies. Various classes of NPs have significantly improved the landscape of therapeutics and applications. Their tunable size, shape and surface chemistry make them highly versatile for drug delivery and precise oncology applications.[1] Their synthesis is broadly classified into two approaches-top down where the larger components are broken down involving techniques such as mechanical milling, lithography, laser ablation, and electrospinning and bottom-up where the smaller particles build up the NPs using methods like sol–gel processing, chemical vapor deposition (CVD), solvothermal and hydrothermal synthesis, or green/biological synthesis routes.[2] Of these, bottom-up approaches using biocompatible resources have emerged as safer and more sustainable strategies for biomedical use.[2,3]

The academic groundwork of nanotechnology is often credited to Richard Feynman's landmark visionary 1959 lecture "There is plenty of room at bottom", which catalyzed global interest in nanomaterials. Since then nanotechnology has rapidly advanced.[4]

More recently Nano medicine focuses on the gravity of multifunctional delivery systems that can overcome challenges of conventional delivery systems such as development of drug resistance, tumour heterogeneity, immunosuppression in tumour microenvironment *etc.* Moreover, NPs are now being functionalised not only as passive targeting agents but also as active agents for immune modulation combination therapy and targeted drug activation.[5]

Colloidal solutions of gold and silver have been used against various diseases since the middle ages.[6] Silver nanoparticles particularly have shown immense potential as therapeutic and theranostic agents. Due to their unique physiochemical properties and efficient biological interaction. AgNPs exhibit broad spectrum anti-microbial and anti-viral, anti-inflammatory and anti-cancer activities, making them valuable in drug delivery, bio sensing, wound healing and cancer therapy applications[7] (REF). Mechanistically AgNPs exert therapeutic effects *via* controlled silver iron (Ag^{+}) release and generation of reactive oxygen species (ROS) which further causes disruption of cellular and mitochondrial membranes and results in cancer cell cytotoxicity and microbial inactivation.[8] However, despite their high therapeutic effect addressing a dose dependent cytotoxicity

[a]*Department of Chemistry, University of Delhi, Delhi-110007, India*
[b]*Department of Biotechnology, Delhi Technological University, Delhi 110042, India*
[c]*Dr B. R. Ambedkar Center for Biomedical Research, University of Delhi, Delhi-110007, India*
[d]*Institute of Nanomedical Sciences (INMS), University of Delhi, Delhi-110007, India*
[e]*Sarojini Naidu Medical College, Agra-28200, Uttar Pradesh, India*
† Equal Contribution.

remains a key concern, underscoring the importance of biocompatible carriers to improve targeted delivery.[9]

Today, NPs are formulated by exploiting various biocompatible resources like proteins, polymers, lipids, *etc.* for applications in disease diagnostics and therapy.[10] One such protein is collagen, abundantly found in connective tissues such as bones, tendons, cartilage, ligaments, and skin as a part of the extracellular matrix to provide mechanical support to the body.[11] Due to its chemical structure, collagen has unique biochemical and biophysical properties like high tensile strength, biodegradability, stretchability, absorption, low immunogenicity, and good safety profile.[11] Due to these physicochemical properties, it has been used as an efficient biomaterial in many medical applications such as wound healing,[12] vascular grafting for coating and delivery of endothelial factors,[13] bone and cartilage reconstruction, damaged skin and cornea healing, urogenital diseases, peripheral nerve migration,[14] and dental applications. Collagen can be easily manipulated into soluble, stable, self-aggregating biomaterials through polymerization to increase mechanical strength and enzymatic resistance. Using various methods and cross-linking agents like physical agents-UV irradiation and dehydrothermal treatment, chemical agents-formaldehyde and glutaraldehyde or more safer crosslinking agents such as chitosan, glucosaminoglycans, elastin *etc.* and enzymatic crosslinking agents-transglutaminase,[15,16] collagen can yield biomaterials of different physical form and applications. A recent novel study reported green synthesis of collagen-base nanoparticles using actinobacteria *Streptomyces xinghaiensis* NEAA-17 and NEAA-3.[18] They were found to be stable and effective in encapsulating methotrexate at loading efficiency of 24.45% and 22.67%, respectively.

Collagen-based nanoparticles (Col-NPs) have been diversely used as delivery vehicles for drugs, proteins, and genes. ColNPs have favorable physical–chemical properties like small size, and large surface area, form colloidal solutions in water, and have increased cell retention.[19] They have been studied as a drug delivery system for improved delivery of a neuroprotective agent, silymarin; they were cross-linked using malondialdehyde (MDA) and 3-ethyl carbodiimide-hydrochloride (EDC-Hcl) and released silymarin sustainably over time.[20] Further, collagen has also been used as a stabilizing agent to cap silver nanoparticles to yield biocompatible and bactericidal AgNP@Collagen of 3.5 nm diameter by irradiating with UV rays.[21] In another study, biocompatible and anti-bacterial AgNP@Collagen were formulated using chemical crosslinking and reducing agents for polymerizing collagen and reducing silver ions, respectively.[22] These AgNP@Col formulations have since been studied either alone[23,24] or modified AgNP@Col with succinylated collagen[24] or in combination with other drugs like plumbagin[25] and doxycycline[26] for wound healing and regeneration.

Noscapine (Nos), is a naturally occurring benzylisoquinoline alkaloid present in the poppy plant or *Papaverum Somniferum* that was initially used as an anti-tussive agent but later was screened for its anti-cancer potential(s).[27] Despite being from a same source as opioids, it is non-toxic, safe, and non-immunogenic as compared to other chemotherapeutics.[28] Nos primarily binds to alpha-tubulin subunits and stabilizes the microtubule polymerization during mitotic spindle fiber formation, blocking metaphase to anaphase transition, thereby inducing apoptosis in the cancerous cell. Nos has been effective against various cancers – breast, lung, prostate, colon cancer, resistant tumors, and in crossing the blood–brain barrier *i.e.* it was found to reduce glioblastomas.[29] However, in pre-clinical and clinical settings, its effectivity becomes limited due to high dose requirement, poor solubility and precipitation in aqueous solution, and absorption.[30]

To improve its solubility and increase its bioavailability in blood, various delivery vehicles have been formulated. These nano-formulations used either metal salts or polymers and proteins or a combination of both to potentially encapsulate noscapine. For instance, Human Serum Albumin (HSA) NPs,[31] poly-lactide-*co*-glycolide (PLGA) NPs,[32] methoxy poly(ethylene glycol)–poly(lactide-*co*-glycolide) NPs (Esnaashari and Amani, 2018), magnetic-based polymeric NPs,[33] PLA, chitosan, PLGA based NPs,[34,35] lipid nanocarriers,[36] PEG-gelatin NPs,[37] silver nanocrystals carrying Nos and reduced-Br-Nos[38] are among the few of the studies that have improved noscapine's solubility. However, most of the nanoparticles synthesized for delivery to a tumor site are obstructed by the dense interstitial matrix that is rich in collagen. Thus, ColNPs encapsulated with anti-cancer agents may be used to effectively infiltrate a tumor site, improving delivery dynamics and therapeutic efficacy of a drug. They are also found to be thermodynamically stable, are efficiently taken up by the cells, and show reduced systemic toxicity.[39] Herein, we study the *in situ* encapsulation of noscapine in multi-component collagen-based silver nanoparticles.

2. Materials and methods

2.1 Chemicals and reagents

All purchased chemicals were used without any further purification. Silver nitrate ($AgNO_3$, 99.0%), sodium borohydride purity ($NaBH_4$ > 96%), and (*S*,*R*)-noscapine (97%) were purchased from Sigma-Aldrich and stored at 2–8 °C. Rat tail collagen I (90%) was purchased from Gibco and was stored at 4 °C. The working solution for Collagen was diluted using 0.1 M acetic acid (purchased from CDH 99.5%) to prepare a final concentration of 0.1 mg mL^{-1}. All solutions and dilutions were prepared in filtered ultra-pure Milli-Q water at room temperature or in the dark wherever necessary. Noscapine was dissolved in HPLC grade DMSO (SRL extrapure 99%).

2.2 Optimization of reaction

Various reaction setups and individual parameters were explored to optimize the procedure of *in situ* loading of noscapine in multicomponent collagen-stabilized silver NPs (Table S1). To begin with, we explored different concentrations and molar ratios of silver nitrate ($AgNO_3$), collagen (Col), and sodium borohydride ($NaBH_4$). The reaction was initially subjected to ultrasonication to facilitate the synthesis of desired NPs, however, the endpoint results were non-reproducible. The reactions were also set up in multiple stages; silver cores were

reduced and coated with collagen which were then collected and used for noscapine encapsulation. The multi-step reaction yielded particles that degraded with each step and passing time. Noscapine hydrochloride salt was also used which degraded over time possibly due to charge destabilization as noscapine-HCl dissociates into noscapine cation and chloride anions. Noscapine (hydrophobic form) was dissolved in different organic solvents out of which DMSO was optimal for our reactions; further different volumes of DMSO were also studied and a minimal amount was used. Finally, the hydrophobic form of noscapine was encapsulated in one pot synthesis of Ag-Col-Nos-NPs.

2.3 Synthesis of Ag-Col-Nos-NPs

Collagen-based silver nanoparticles were synthesized using a previously reported method with slight modification.[22] The method was modified to accommodate one-pot synthesis of noscapine-loaded collagen-based silver nanoparticles (Ag-Col-Nos-NPs). 0.1 M collagen was dissolved in 0.1 M acetic acid by stirring constantly for 30 minutes at room temperature. 0.08 M of noscapine dissolved in DMSO was added dropwise to the reaction at constant stirring. After 30 minutes of stirring, 0.1 M of silver nitrate solution was added dropwise and kept further for stirring for 30 minutes. A freshly prepared 0.2 M solution of $NaBH_4$ in ice-cold water was prepared and carefully added at one drop per second to the reaction and stirred further for 10 minutes. The final solution was transferred to a falcon and centrifuged at 10 000 rpm for 10 minutes. The obtained pellet was resuspended and washed with Milli-Q to remove the unreacted reactants. The final collected pellet was lyophilized and stored for characterized and biological evaluation. The reaction and the pellet were kept away from direct light exposure (Fig. 1).

3. Characterization of nanoparticles

3.1 Ultraviolet-visible spectroscopy

One of the most preliminary techniques to examine the formation of AgNPs is UV-visible spectrometry. The spectrum was recorded within a scan range of 200–600 nm in a quartz cuvette of 1 cm path length at room temperature using Thermo Scientific's Evolution 300 spectrophotometer. To visualize a comparison, spectra of Nos (90 μM), AgNPs, and Ag-Col-NPs were also taken within the same range and parameters. The spectra were recorded plotted and overlayed with wavelength on the *x*-axis and absorbance on the *y*-axis using origin software.

3.2 Dynamic light scattering and zeta potential

Dynamic Light Scattering (DLS) technology wherein speckle pattern produced by the diffusing particles is detected by a photodiode detector Zetasizer generating a correlation function which is further analysed into an average hydrodynamic size of the particle. DLS technique was employed to examine the mean particle size and surface charge of the Ag-Col-Nos-NPs using a Zetasizer Nano-ZS (Malvern Instruments, Malvern, UK), employing a He–Ne laser (5 mW) operating at 633 nm wavelength. Samples were freshly prepared and sonicated before carrying out the analysis.

3.3 Transmission electron microscopy

Transmission electron microscopy was performed using TECNAI 200 kV transmission electron microscope (FEI, Electron Optics) for morphological evaluation and size determination of Ag-Col-Nos-NPs and AgNPs for comparison. A drop cast of Ag-Col-Nos-NPs and AgNPs was done over a carbon carbon-coated grid and was kept for overnight drying at room

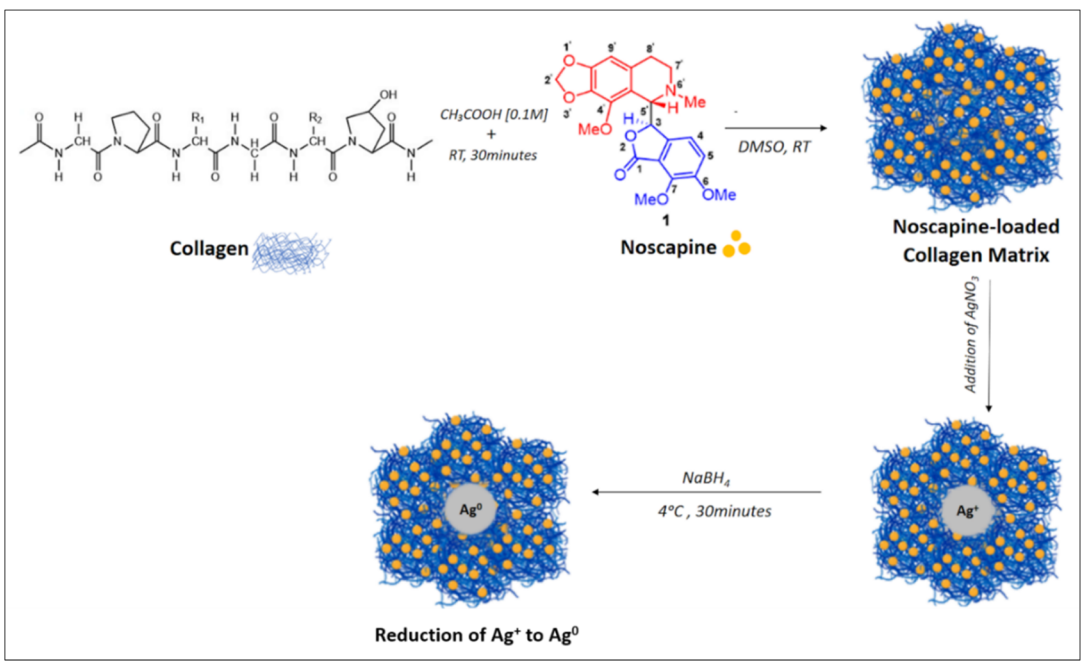

Fig. 1 Schematic representation of synthesis of Ag-Col-Nos-NP.

temperature. The prepared grid was used for visualization *via* TEM.

3.4 Field emission scanning electron microscopy (FeSEM) analysis

For detailed surface morphological analysis, Field Emission Scanning Electron Microscopy was conducted using Gemini SEM 500 (Carl Zeiss, Germany). A nanoparticle suspension of Ag-Col-Nos was prepared, and a drop of this suspension was drop cast onto a clean glass slide and left to dry overnight at RT to form a thin uniform film. The dried slide was visualised under FeSEM. Images were captured at 100 nm and 20 nm magnification to examine particle morphology, surface texture, and dispersion characteristics.

3.5 X-ray diffraction

Structure determination and XRD patterns of Ag-Col-Nos-NPs and AgNPs were performed using Bruker D8 Discover X-ray diffractometer equipped with Cu, 3 kW as the X-ray source, and Eulerian cradle with 6 degrees of freedom sample stage. Scanning from a range of 5° to 80° with a step size of 0.02° generated diffraction patterns which were recorded, treated, and plotted using origin software.

3.6 Energy-dispersive X-ray spectroscopy (EDS)

Elemental analysis of nanoparticles was done using JEOL: JSM 6610LV, energy dispersive X-ray spectroscopy (EDS). The percentage weight and atomic composition of each element in the final Ag-Col-Nos-NPs-NPs were recorded.

3.7 Fourier-transform infrared (FTIR)

The functional groups of lyophilized nanoparticles, noscapine, and collagen were analyzed and compared using Thermo Scientific Nicolet iS50 Fourier-Transform Infrared Tri-detector Spectrophotometer. The spectra were recorded at room temperature in the spectral range frequency of 400–4000 cm^{-1} by the KBr disc method.

3.8 Determination of drug loading efficiency

Absorbance of noscapine at different (increasing) concentrations was recorded in the UV region using a Thermo Scientific's Evolution 300 spectrophotometer. The absorbance at λ_{max} (311 nm) was then plotted with respective concentration (0–225 μM) on the *x*-axis, and the data was fit into a straight-line equation to generate a standard curve of noscapine. The absorbance of the purified pellet was recorded and plotted in the standard curve produced to analyze the % Drug Loading Efficiency (DLE) of noscapine entrapped in the Ag-Col-Nos-NPs as per the following formula:

$$\text{Drug loading efficiency } \% = \frac{\text{Amount of Nos loaded}}{\text{Initial amount of Nos}} \times 100$$

3.9 *In vitro* noscapine release kinetics

The *in vitro* drug release profile of both Ag-Col-Nos NPs and free noscapine individually was examined using dialysis bag. A 12 000 Da MWCO regenerated cellulose membrane (Sigma-Aldrich, Cat# D6191-25EA) was pre-soaked in Milli-Q water before use.

The dialysis bag was loaded with 5 mL of 1 mg mL^{-1} of nanoparticles suspension in parallel with a 10 mg mL^{-1} solution of noscapine dissolved in DMSO. Each dialysis bag was suspended in 400 mL of phosphate-buffered saline (PBS, pH 5.5 & 7.4) to mimic tumor microenvironment and physiological pH. The entire setup was maintained at 37 °C with constant stirring at 50 rpm. At specific time intervals (1 to 72 hours), 2 mL of release medium was withdrawn and replaced with fresh 1× PBS. The concentration of noscapine released into the medium was quantified by UV-Vis spectrophotometry at 311 nm, using a standard calibration curve prepared under identical buffer conditions (Fig. 2).

Total drug release in the medium was calculated using

$$\%\ \text{Drug release} = \frac{\text{Drug released in medium}}{\text{Total drug concentration}} \times 100$$

4. Biological evaluation

4.1 Cell culture

Non-small cell lung cancer cell line-H1299 was purchased from NCCS Pune. The cells were cultured in Dulbecco Eagle's modified medium (DMEM, Himedia) supplemented with 10% fetal bovine serum (FBS, Himedia) and 1% of antibiotic–antimycotic cocktail (100×, Gibco). The cells were maintained in a humidified incubator with 5% CO_2 at 37 °C.

4.2 MTT cytotoxicity assay

4.2.1 Preparation of stock solutions. The stock solution of Ag-Col-Nos-NPs with a concentration of 1 mg mL^{-1} was prepared in filtered Milli-Q water whereas a stock of noscapine was made in dimethyl sulfoxide respectively for comparative cell viability analysis.

4.2.2 Concentration-dependent cytotoxic study. The cells were harvested from a T-75 cm^2 culture flask and seeded in a 96-well plate with a cell density of 1×10^4 cells per well. The cells were placed in a humified incubator at 5% CO_2 overnight and were treated with gradient concentrations of Ag-Col-Nos-NPs and noscapine the next day. The variable concentrations of Ag-Col-Nos-NPs were kept in a range of 0–200 μg mL^{-1}. The cells were treated for 48 hours and 72 hours in triplicate technical as well as biological repeats and normalized with control cells. For noscapine, 1% DMSO was used as the control group. After respective treatments, the drug was removed from the wells, and the cells were incubated with 0.5 mg mL^{-1} of MTT (3-[4,5-dimethylthiazol-2-yl]-2,5 diphenyl tetrazolium bromide) dye. Each well was supplied with 100 μL of 0.5 mg per mL MTT solution. The cells were then incubated in a humidified incubator at 5% CO_2 for 3–4 hours. Thereafter, the MTT solution was

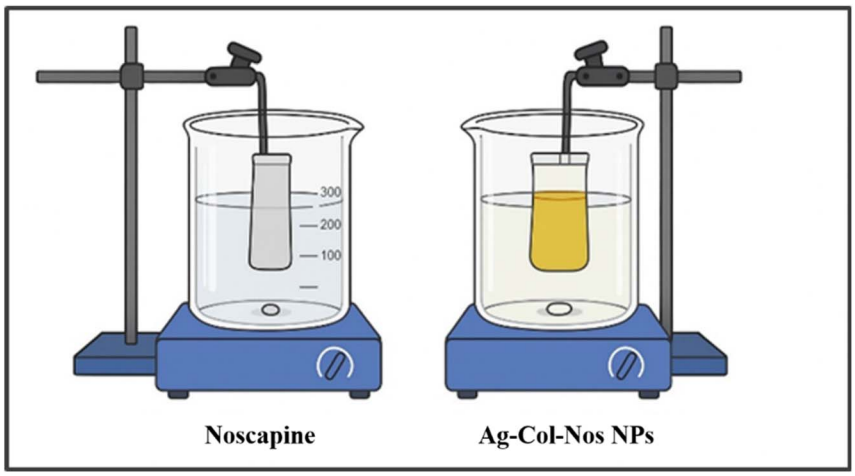

Fig. 2 Experimental setup of *in vitro* release study using dialysis.

aspirated, and the formed crystals were dissolved in 100 μL of DMSO in each well. Absorbance was recorded using Tecan infinite M200 multi-plate reader at a wavelength of 570 nm. The percentage of viable cells was plotted as a function of drug concentration to compare the treated groups with the control group and determine the IC_{50} value. The study was performed in three biological and three technical repeats.

5. Results and discussion

The study aimed to synthesize safe, effective biocompatible nanoparticles with a better ability to reach a cancerous cell to deliver noscapine. Herein, we developed a modified procedure of one-pot synthesis of collagen-based silver NPs to encapsulate noscapine. Collagen was used both as a stabilizer and a drug delivery vehicle. Collagen is found in abundance in extracellular matrix and hence it provides membrane solubility and makes it a potential biomolecule for drug delivery. One of the issues faced by many targeted NPs is the inability to cross the extensive ECM network surrounding a cancer cell; a collagen-based NP formulation is unlikely to be hindered by such an environment of cells.

5.1 Synthesis of Ag-Col-Nos-NPs

The synthesis of nanoparticles was carried out using a modified protocol already reported for collagen-coated silver nanoparticles.[22] The synthesis was carried out at room temperature under constant stirring. No precipitate was observed upon the addition of individual reagents anytime during the reaction. $NABH_4$ was freshly prepared and stored at a low temperature (4 °C) until its addition in the last step of the reaction. The subsequent addition of ice-cold $NaBH_4$ caused a gradual change in the colour of the reaction from transparent to light yellow and to yellowish brown on further addition of $NaBH_4$, indicating the formation of silver nanoparticles (Fig. 3). The pelleted-down particles were brown coloured, stable at room temperature, and 4 °C degrees when kept overnight.

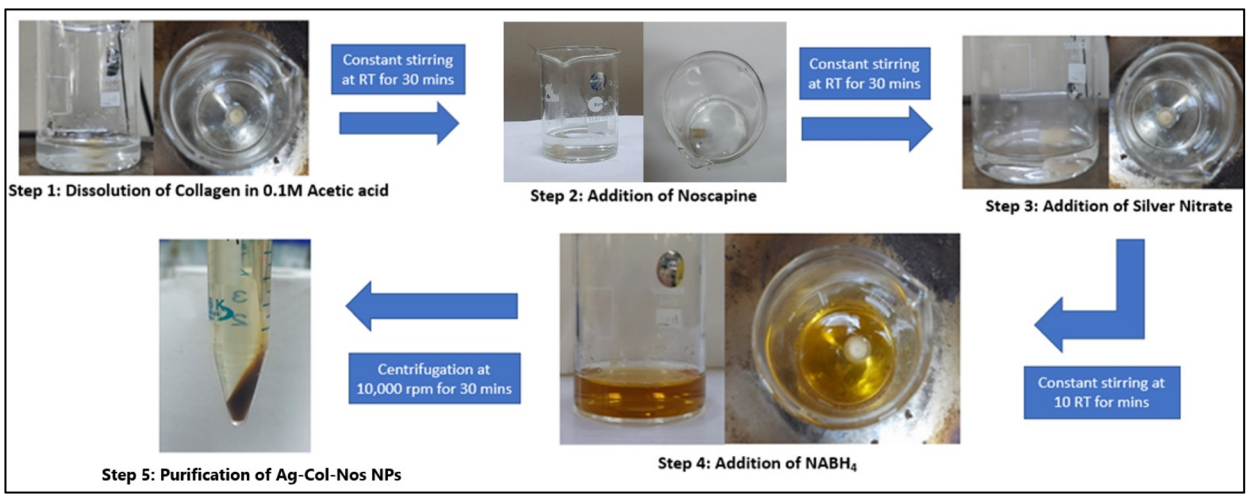

Fig. 3 Representation of the procedure for synthesis of Ag-Col-Nos-NPs.

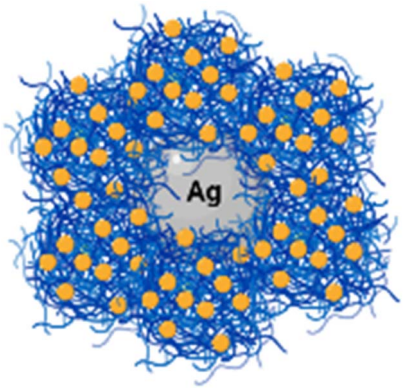

Fig. 4 Theoretical representation of Ag-Col-Nos-NPs.

We achieved a water-soluble nanoformulation and overcame the challenge of drug precipitation in the aqueous environment. It was hypothesized that the Ag-Col-Nos-NPs nanoparticles had a silver centre which was surrounded by the collagen molecules interlinked making hydrophobic cores wherein Nos molecules were entrapped (Fig. 4). The purified pellet was completely homogenized in water and was stable for up to three months as evidenced by the UV-Vis spectra and DLS measurements.

5.2 Spectroscopy analysis

UV-visible spectroscopy provides preliminary confirmation of the formation of AgNPs as they emit a characteristic spectrum (λ_{max}) due to surface plasmon resonance (SPR) in the UV region. This λ_{max} varies with the size of the AgNPs; the increase in size

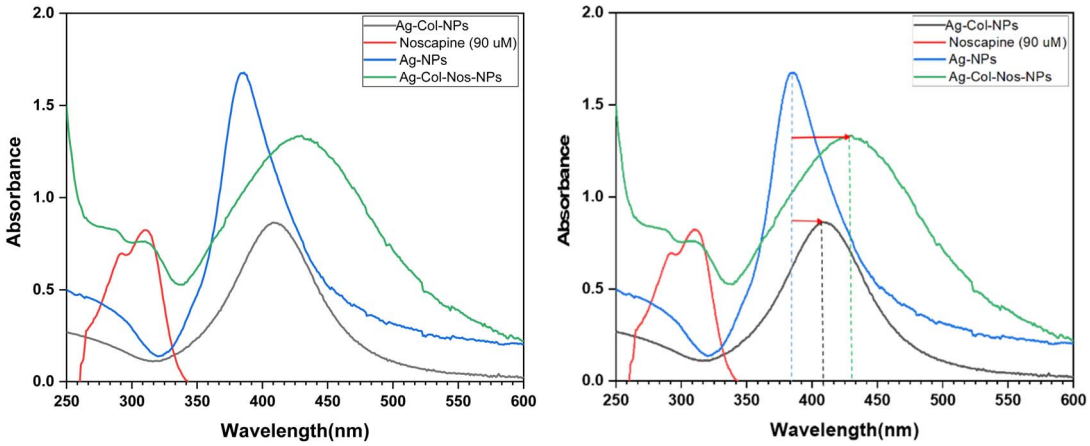

Fig. 5 UV-visible spectroscopy: a shift toward a higher wavelength was observed for Ag-Col-Nos-NPs with a λ_{max} at 430 nm indicating an increase in size of the core Ag-NPs.

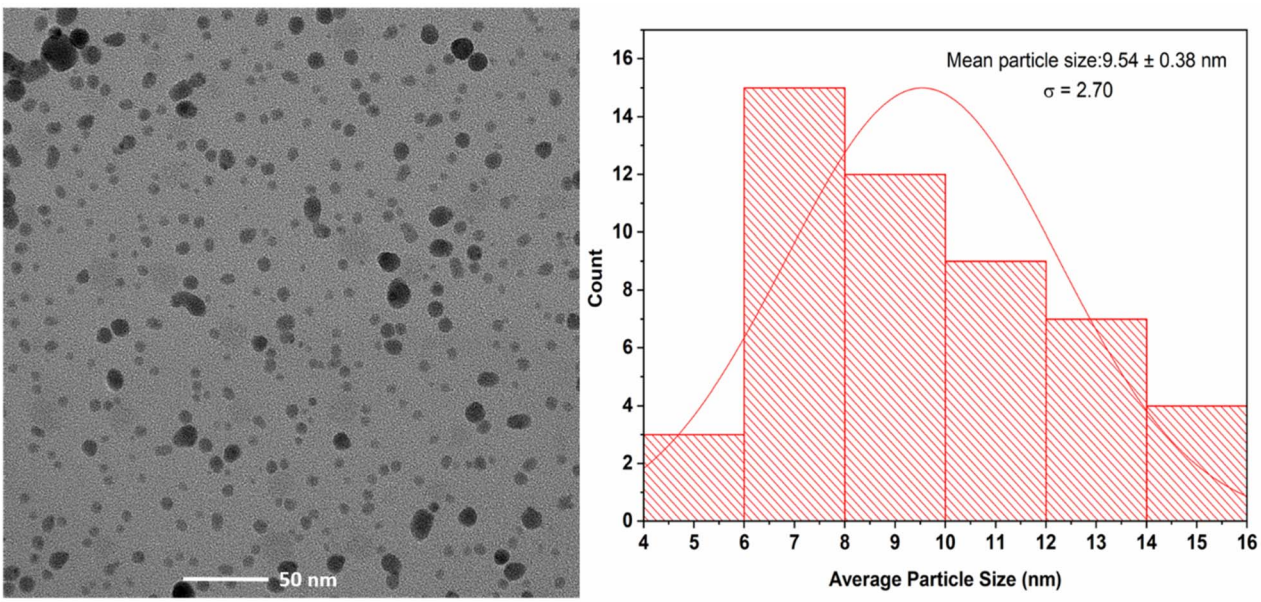

Fig. 6 Size and shape analysis of Ag-Col-Nos-NPs by TEM measurements (scale: 50 nm).

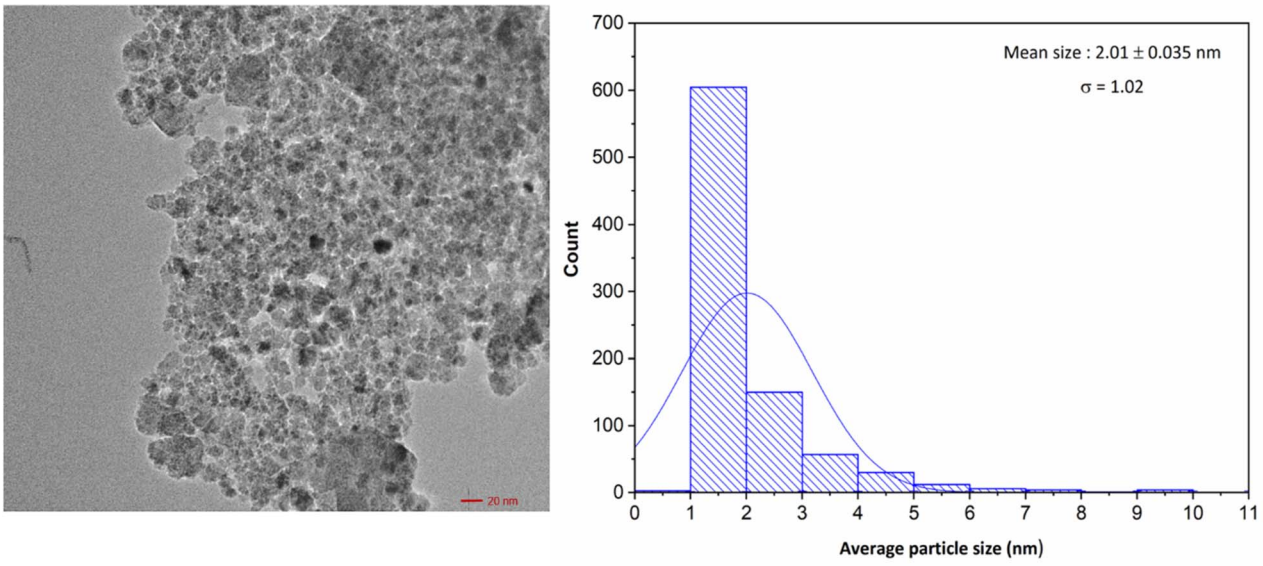

Fig. 7 Size and shape analysis of AgNPs by TEM measurements (scale 20 nm).

corresponds to an increase in λ_{max}. The optical properties of the free noscapine, AgNP, Ag-Col-NPs, and Ag-Col-Nos-NPs were measured using a UV-Vis spectrophotometer. The yellow-brown colour indicative of the formation of Ag-Col-Nos-NPs showed a sharp peak at 430 nm, confirming the formation of Ag-Col-Nos-NPs (Fig. 5). A progressive red shift in the SPR peak was observed from 385 nm (AgNPs) to 405 nm (Ag-Col-NPs) and 430 nm (Ag-Col-Nos-NPs). This red shift indicates an increase in particle size due to collagen coating and noscapine loading. Additionally, the broader peak observed for Ag-Col-Nos-NPs suggests increased polydispersity. A distinct absorption peak at 311 nm in the spectrum of Ag-Col-Nos-NPs corresponds to the presence of noscapine, confirming its successful incorporation.

5.3 Size, shape and surface charge analysis

The mean particle size of the Nos-loaded silver-coated collagen nanoparticles was 211.3 nm with a polydispersity index of 0.133. The Ag-Col-Nos NPs exhibited a zeta potential of +6.60 mV, indicating a positive surface charge (Fig. 9). The particles were stable at room temperature with negligible change in the average size for up to three months. Since DLS is limited to providing only hydrodynamic size (*i.e.* how the size of particular molecule behaves in presence of water), to assess the precise size and shape, Ag-Col-Nos-NPs and AgNPs were visualized using high-resolution images produced by TEM. The images produced with a 50 nm and 20 nm scale respectively were then analysed for the average particle size through Image J software and a histogram was plotted to calculate the average size as 9.54 nm (Fig. 6). The shape of the Ag-Col-Nos-NPs synthesized was primarily found to be spherical and otherwise irregular shapes were also observed. Meanwhile, AgNPs showed spherical morphology with an average particle size of approximately 2.01 nm (Fig. 7). Although significant aggregation of the nanoparticles was observed which is likely due to the high surface

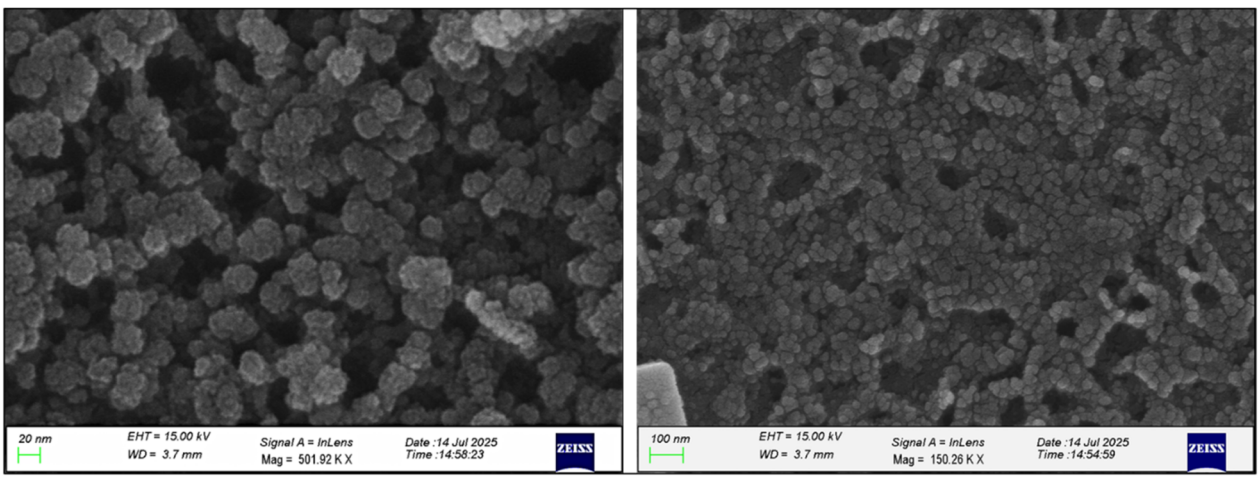

Fig. 8 Fe-SEM measurements of Ag-Col-Nos NPs at 20 nm and 100 nm.

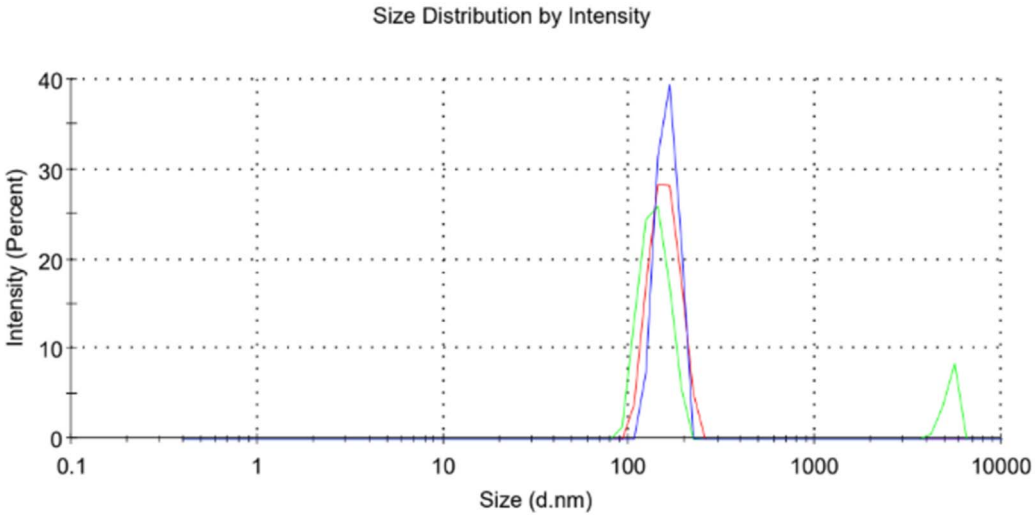

Sample	Avg. zeta potential	Temperature	Poly dispersity Index (PDI)	Diameter d (nm)	Solvent
Ag-Col-Nos	6.60	25°C	0.133	211.3	Water

Fig. 9 Zeta potential distribution image of synthesized Ag-Col-Nos NPs.

energy and the absence of any additional stabilizing agents or surface capping molecules resulting in insufficient electrostatic repulsion between the particles.[40,41] Therefore, in our synthesized formulation collagen (Col) was employed as a biocompatible stabilizing agent. The introduction of collagen provided a capping effect, reducing particle aggregation by imparting steric hindrance and possible surface charge stabilization.

However, we see particles of various sizes, indicating a polydisperse formation, as would be expected with the use of a biomolecule wherein it is tricky to control the size of the particles, confirming our observation from UV spectra. The small size observed is ideal for efficient transport, penetrating tissues, cellular uptake, and the ability to be modified for better cell-specific targetability. These advantageous properties make them attractive nano-formulations for drug delivery.

5.3.1 Field emission scanning microscopy analysis. Field emission scanning microscopy analysis was performed to analyse the surface morphology and structure of synthesized Ag-Col-Nos NPs. The obtained result (Fig. 8) shows the formation of spherical and uniformly distributed nanoparticles. The surface of Ag-Col-Nos NPs appeared smooth with mild agglomeration due to relative surface charge and presence of collagen.

The average particle size as observed by TEM is further confirmed as it lies within the nanometre range. Further the

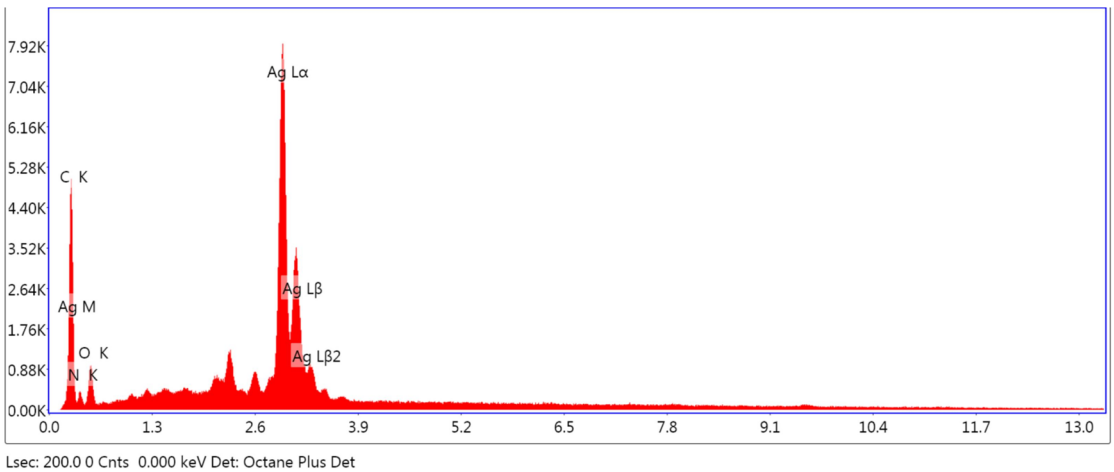

Fig. 10 Elemental analysis of Ag-Col-Nos-NPs.

consistent morphology reveals the effective stabilisation of NPs through collagen preventing aggregation and size revealed the structural morphology of nanoparticles within 20 nm of range.

5.4 Elemental analysis

The elemental analysis provides crucial insights into the composition of the Ag-Col-Nos-NPs. A prominent peak in silver indicates the substantial presence of silver in the synthesized nanoparticles. Furthermore, the characteristic signals of carbon (C), nitrogen (N), and oxygen (O), confirm the presence of collagen and noscapine.

The obtained percentage composition reveals the relative amounts of each element, with silver comprising 69.8 wt%, oxygen at 15.21 wt%, carbon at 11.44 wt%, and nitrogen at 3.54 wt%. These findings are consistent with the expected structural composition of the synthesized nanoparticles, validating the accuracy of the proposed formulation. The elemental analysis not only confirms the incorporation of silver and collagen but also provides quantitative data supporting the overall structural integrity of Ag-Col-Nos-NPs (Fig. 10).

5.5 Analysis of surface functionalities

Surface functionalities of the nanoparticles (NPs) were investigated through Fourier Transform Infrared (FTIR) spectroscopy, employing Ag-Col-Nos-NPs, collagen, and noscapine as the subjects. FTIR spectroscopy measures the wavelength and intensity of infrared absorption by the sample, producing spectra that reveal molecular vibrations characteristic of specific features in the compound, aiding in their identification. Each bond or structural feature of a compound or biological molecule yields a specific spectrum in the infrared (IR) region.

The IR spectrum of pure collagen distinctively shows an amide I bond at 1641 cm^{-1} which was seen to shift in wavelength and decrease intensity in Ag-Col-Nos-NPs, indicating the involvement of C=O in AgNP stabilization. Similarly, Ag-Col-Nos-NPs show characteristic peaks of noscapine as visible in the overlapped spectra between 1500 and 700 cm^{-1} (Fig. 11). The reduced intensity and shift in collagen and noscapine peaks indicate their involvement in facilitating interaction, reinforcing the understanding of the surface functionalities in the synthesized nanoparticles.

5.6 XRD measurements

XRD pattern of AgNPs shows four distinct diffraction peaks at 38.49°, 44.73°, 64.91° and 78.88° at 2θ values. However, Ag-Col-Nos-NPs show an amorphous peak as reported previously for Ag-Col-NPs[15] (Fig. 12). This indicates that the silver centre is encompassed by the collagen molecules.

5.7 Drug loading efficiency (DLE)

To quantify the number of Nos molecules entrapped in the Ag-Col-Nos-NPs, drug loading efficiency (DLE) was calculated using UV-Vis Spectroscopy.[42] DLE can essentially be defined as the ratio of the amount of Nos loaded to the amount of Nos initially used. The number of Nos loaded was determined by taking a UV spectrum of the purified Ag-Col-Nos-NPs pellet and put into a standard curve plotted for various UV absorbance of Nos (0–225 μM; $r^2 = 0.9964$).[43] DLE was calculated to be about 14.5% *i.e.*, about 14.5 molecules of Nos were loaded per protein which is more than what is reported for most nanoparticle delivery systems; most nanoparticles show a drug loading capacity of less than 10%.[44]

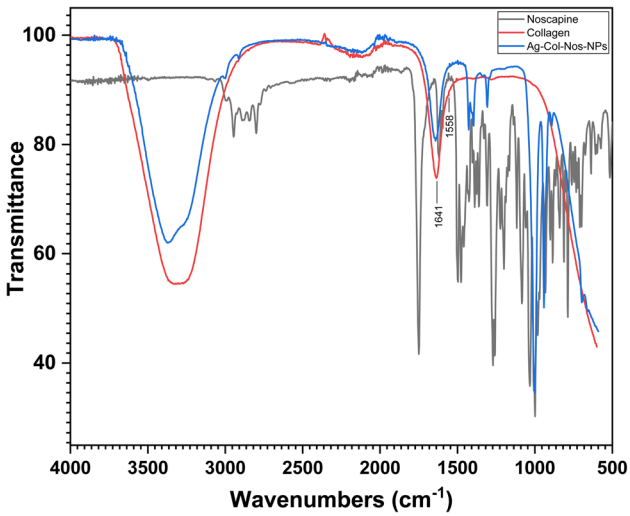

Fig. 11 FTIR Measurement: comparison of the IR spectra of collagen, noscapine and Ag-Col-Nos-NPs.

5.8 *In vitro* noscapine release kinetics

The *in vitro* release profiles of Ag-Col-Nos NPs and free noscapine were studied at both acidic (pH 5.5) and physiological (pH 7.4) conditions over a 72-hour period. Ag-Col-Nos NPs showed a sustained and pH-responsive release (Fig. 13). At pH 5.5, approximately 65% of noscapine was released by 72 hours,

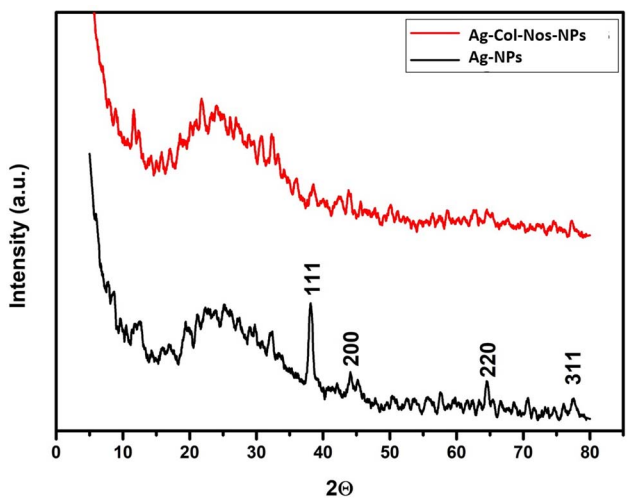

Fig. 12 XRD measurements for Ag-Col-Nos-NPs (red) and Ag-NPs (black).

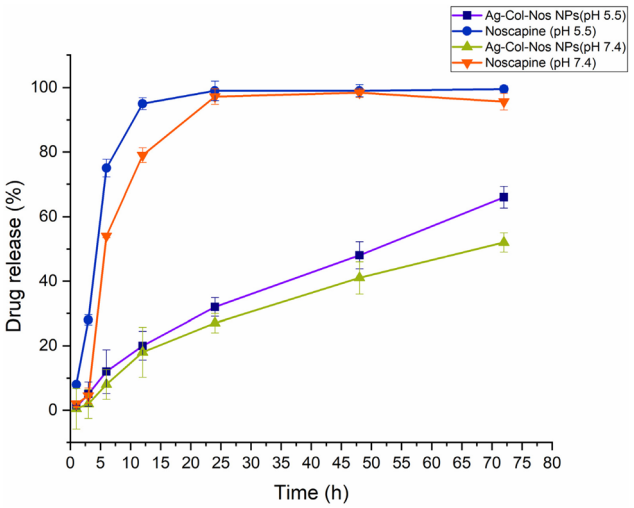

Fig. 13 *In vitro* drug release profiles of free noscapine and noscapine encapsulated in Ag-Col-Nos NPs at pH 5.5 and pH 7.4 over 72 hours. Data are presented as mean ± standard deviation ($n = 3$).

whereas a significantly slower release of 52% was observed at pH 7.4 in the same period.

In contrast, free noscapine demonstrated a burst release at both pH levels. There was a slightly higher release at pH 5.5 within the first 12 hours compared to pH 7.4, indicating improved aqueous solubility and diffusion of free noscapine under acidic conditions.[37]

Noscapine, a weakly basic drug with a pK_a of approximately 7.8, exhibits pH-dependent ionization. At lower pH (*e.g.*, 5.5), which is below its pK_a, noscapine becomes predominantly protonated and more ionized. This ionized form generally improves its aqueous solubility. Conversely, at physiological pH (7.4), while still significantly ionized, the proportion of the unionized form is higher compared to more acidic conditions. This shift in ionization, coupled with the properties of the Ag-Col-Nos NPs matrix, influences drug release.[37]

Our findings observe that the Ag-Col-Nos NPs act as a controlled release system. This pH-responsive behaviour is particularly advantageous for tumor-targeted therapy, where acidic microenvironments are common. Further, Ag-Col-Nos NPs aids noscapine's solubility limitations by enabling slow and sustained release, reducing the initial burst effect seen with the free drug. This controlled delivery may contribute to enhanced cytotoxicity in acidic tumor-mimicking environments by ensuring continuous drug release at the target site while minimizing systemic drug accumulation.

5.9 Solubility and stability of nanoparticles

It was observed that purified Ag-Col-Nos-NPs (1 mg mL^{-1}) dissolved in an aqueous medium whereas noscapine (1 mg mL^{-1}) did not dissolve in an aqueous medium. 1 mg mL^{-1} solution of Ag-Col-Nos-NPs kept in an Eppendorf for an extended period did not show any aggregation or precipitation at room temperature. This indicates efficient solubility and stability of Ag-Col-Nos-NPs than noscapine in aqueous solution and supports the incorporation of noscapine in Ag-Col-NPs.

5.10 Anti-cancer activity of nanoparticles

This study aimed to synthesize a nano-formulation to increase the bioavailability of Nos since Nos is excreted out of the body quickly. Herein, we evaluate if these nano-formulations would aid in the sustained release of noscapine in response to time when compared to cells treated with only Nos. We used a non-small cell lung cancer cell line-H1299. Cells were seeded in a 96-well plate and grown overnight. The next day, cells were treated with various concentrations of Nos and Ag-Col-Nos-NPs and incubated for 48 hours and 72 hours. After incubation, the cells were removed from the incubator and supplemented with MTT dye at 0.5 mg mL^{-1} final concentration. The plates were further incubated for 3 hours in the humidified incubator at 5% CO_2. Following incubation with MTT, the formed crystals were dissolved in DMSO. The spectral readings taken were normalized

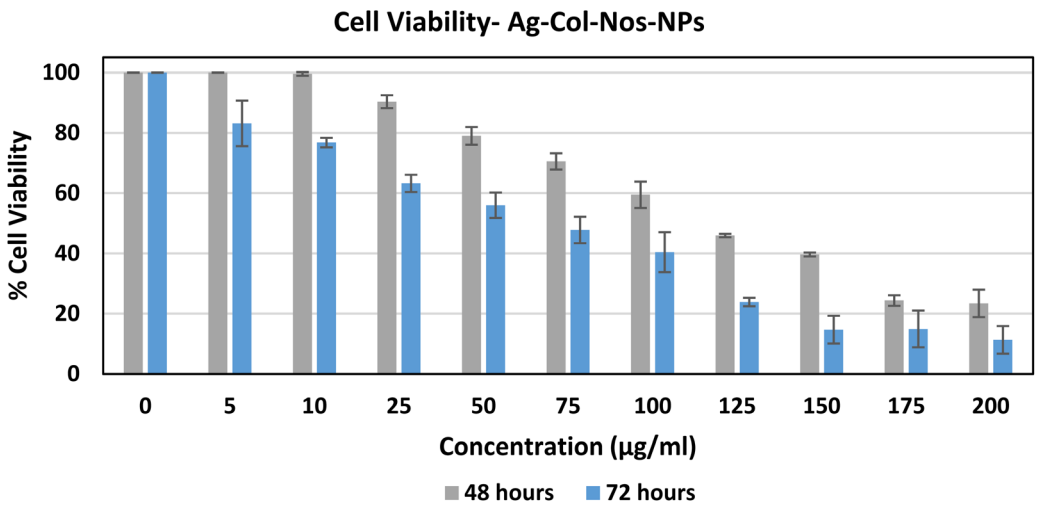

Fig. 14 Dose-dependent cytotoxicity of Ag-Col-Nos nanoparticles on H1299 cells evaluated by MTT assay at 48 and 72 hours. Results indicate sustained and time-dependent inhibition of cell viability.

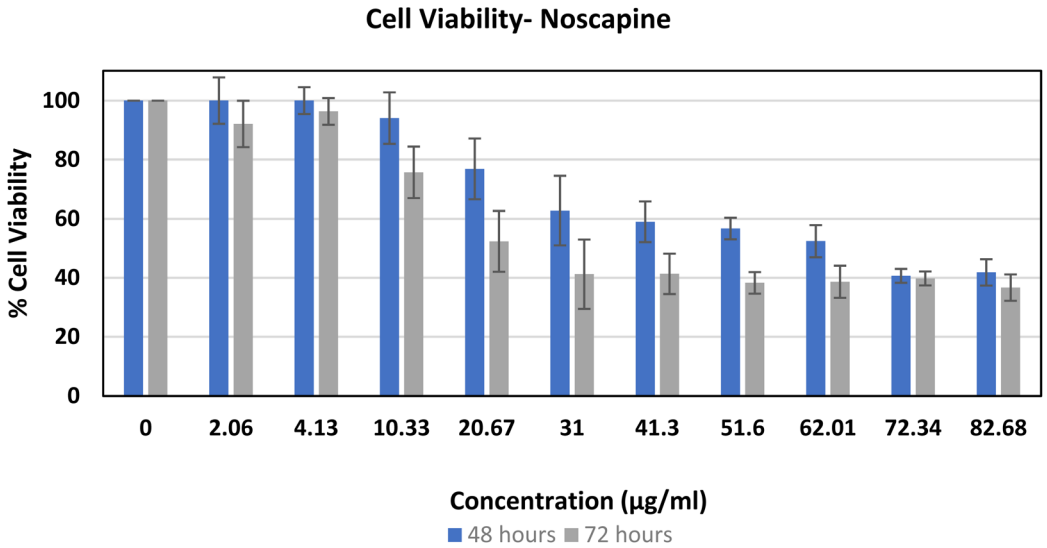

Fig. 15 Dose-dependent cytotoxicity of free noscapine on H1299 cells evaluated by MTT assay at 48 and 72 hours. Compared to Ag-Col-Nos-NPs, a higher variation in viability was observed suggesting burst release.

and plotted against concentration (Fig. 14 and 15). At 48 hours and 72 hours, the IC_{50} calculated for Ag-Col-Nos-NPs was 123 µg mL^{-1} and 79.29 µg mL^{-1}, respectively.

The anti-proliferation activity of noscapine and Ag-Col-Nos-NPs is comparable; however, it was observed that the percentage of cell viability for Ag-Col-Nos-NPs (Fig. 14) showed less variability from the mean compared to treatment with noscapine alone (Fig. 15), suggesting a gradual time dependent cytotoxicity (Fig. 15). It has been reported that Ag-Col-NPs show no cytotoxicity in *in vitro* models of breast cancer cell lines

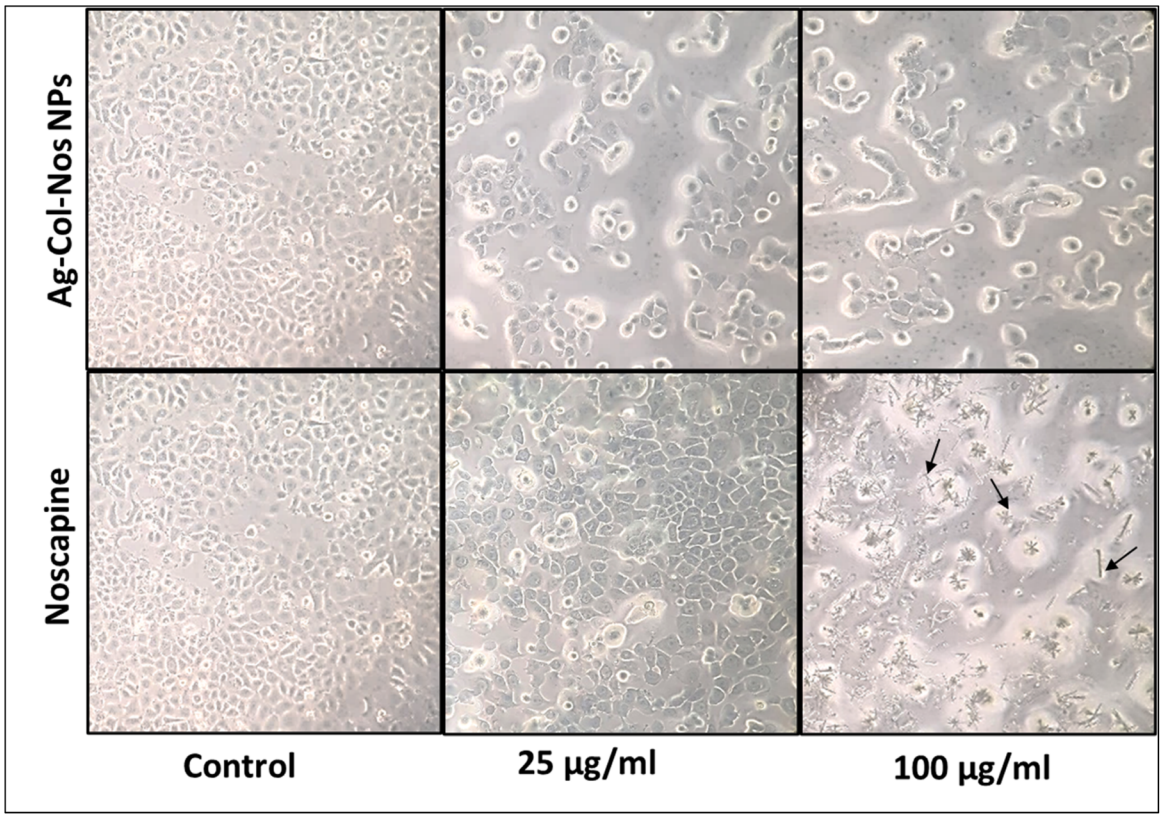

Fig. 16 Light microscopy (10×) images showing precipitation of noscapine in aqueous solution. The arrows show the precipitated drug after 48 hours of treatments.

(MDA-MB-23).[22,44] Further, we observe the sustained release of noscapine from Ag-Col-Nos-NPs over an extended period. Noscapine is a hydrophobic drug with reduced solubility and absorption; it precipitates in an aqueous solution[45] as we observed during our MTT experiment as well (Fig. 16). However, cells treated with Ag-Col-Nos-NPs do not show any precipitation even after 72 hours. Therefore, *in situ* encapsulation of noscapine in Ag-Col-Nos-NPs, shows anti-proliferation activity with sustained release and no precipitation, increasing the solubility of noscapine in a slightly alkaline aqueous environment.

6. Limitation of the study

While the results of this study are promising but may be considered with some possible limitations. First, a low drug loading efficiency was observed with the proposed formulation technique. The use of efficient cross-linking agents may aid collagen inter-bonding to entrap drug molecules. Secondly, much of the time and resources of the already limited funds were spent on optimizing the reported procedure for synthesis of Ag-Col-Nos-NPs which resulted in limited available final material for additional characterization. Thirdly, unavailability of animal facilities to study the pharmacokinetics of the formulated Ag-Col-Nos-NPs. This preliminary study may advance into the formulation of efficient hydrophilic and safe collagen particles for the delivery of anti-cancer hydrophobic drugs like noscapine. In addition, due to the lack of access to specialized 3D tumor culture systems, the ECM-penetration and tumor-targeting potential of collagen could not be experimentally validated in this study. This preliminary work may advance into the formulation of efficient, hydrophilic, and non-toxic collagen particles for the delivery of anti-cancer hydrophobic drugs like noscapine.

7. Conclusion

Noscapine (Nos) is an anti-cancer agent that has been researched extensively for its potent anti-proliferative activities and very valuable non-toxic, non-immunogenic, and safe properties. However, one of its major disadvantages is its short half-life, which essentially translates into quick excretion of Nos from the body. To overcome this, herein we successfully encapsulated Nos in collagen-based silver nanoparticles. Collagen is a protein that is naturally available in the body-its unique nature of intercalating through the formation of hydrogen bonds and making hydrophobic pockets in aqueous solution makes it a suitable agent for drug delivery for sustainable release. The synthesized Ag-Col-Nos-NPs were 9.54 nm in size and were mostly spherically shaped. Elemental studies confirmed the presence of Ag in the synthesized NPs whereas XRD showed a diffraction pattern of an amorphous compound confirming the coating of the silver center with collagen. Finally, FTIR confirmed the presence of noscapine in the nano-formulation. *In vitro* drug release studies showed sustained and pH-responsive noscapine release, while cytotoxicity assays demonstrated effective, time-dependent anti-proliferative activity on H1299 lung cancer cells without precipitation. Collectively, these findings suggest that Ag-Col-Nos-NPs represent a promising nano-therapeutic platform for improving the solubility, stability, and bioavailability of noscapine and potentially other hydrophobic anti-cancer agents.

Author contributions

H. C., N. M. and R. C. contributed to the idea or design of the work. H. C. and N. M. performed the nanoparticle synthesis, characterization, biological evaluation, analysis and interpretation of data for the work. H. C., N. M., S. C., J. S. and R. C. contributed to the drafting of the work, reviewing the intellectual content of the manuscript. R. C. and J. S. reviewed the final compilation of work and revisions. All authors have agreed to the final version, helped in analysis of the data and provided critical feedbacks during the writing and revision of the manuscript.

Conflicts of interest

There is no conflict of interest among authors.

Abbreviations

Ag-Col-Nos NPs	Silver-based collagen nanoparticles loaded with noscapine
AgNPs	Silver nanoparticles
Col-NPs	Collagen-based nanoparticles
DMSO	Dimethyl sulphoxide
Nos	Noscapine
MTT	3-(4,5-Dimethylthiazol-2-yl)-2,5-diphenyltetrazolium bromide
IC_{50}	Half maximal inhibitory concentration
DMEM	Dulbecco's modified Eagle's medium

Data availability

The datasets supporting the findings of this study are available from the corresponding author upon request.

All data generated or analyzed during this study are included in the article and its SI files, where applicable. See DOI: **https://doi.org/10.1039/d5ra03766b**.

Acknowledgements

Prof. Ramesh Chandra thankfully acknowledges DBT (BT/PR36874/MED/97/475/2020) for financial assistance. The researchers acknowledge the staff and facilities at the Department of Chemistry, University of Delhi for their support and guidance. Heerak Chugh extends her sincere gratitude to the Indian Council of Medical Research for the Senior Research Fellowship. Nistha Mishra extends her gratitude to Department of Biotechnology, Delhi technological University for providing fellowship.

References

1 J. J. Giner-Casares, M. Henriksen-Lacey, M. Coronado-Puchau and L. M. Liz-Marzán, Inorganic nanoparticles for biomedicine: where materials scientists meet medical research, *Mater. Today*, 2016, **19**(1), 19–28.
2 N. Baig, I. Kammakakam and W. Falath, Nanomaterials: a review of synthesis methods, properties, recent progress, and challenges, *Mater. Adv.*, 2021, **2**(6), 1821–1871.
3 I. Roy, Therapeutic applications of magnetic nanoparticles: recent advances, *Mater. Adv.*, 2022, **3**(20), 7425–7444.
4 S. Bayda, M. Adeel, T. Tuccinardi, M. Cordani and F. Rizzolio, The history of nanoscience and nanotechnology: from chemical–physical applications to nanomedicine, *Molecules*, 2019, **25**(1), 112.
5 R. M. Joshi, B. Telang, G. Soni and A. Khalife, Overview of perspectives on cancer, newer therapies, and future directions, *Oncol. Transl. Med.*, 2024, **10**(3), 105–109.
6 H. Chugh, D. Sood, I. Chandra, V. Tomar, G. Dhawan and R. Chandra, Role of gold and silver nanoparticles in cancer nano-medicine, *Artif. Cells, Nanomed., Biotechnol.*, 2018, **46**(sup1), 1210–1220.
7 S. Singh, T. Goel, A. Singh, H. Chugh, N. Chakraborty, I. Roy, *et al.*, Synthesis and characterization of Fe_3O_4@SiO_2@PDA@Ag core–shell nanoparticles and biological application on human lung cancer cell line and antibacterial strains, *Artif. Cells, Nanomed., Biotechnol.*, 2024, **52**(1), 46–58.
8 N. Chatterjee, S. Pal and P. Dhar, Green silver nanoparticles from bacteria – antioxidant, cytotoxic and antifungal activities, *Next Nanotechnol.*, 2024, **6**, 100089.
9 M. Harun-Ur-Rashid, T. Foyez, S. B. Krishna, S. Poda and A. B. Imran, Recent advances of silver nanoparticle-based polymer nanocomposites for biomedical applications, *RSC Adv.*, 2025, **15**(11), 8480–8505.
10 R. Song, M. Murphy, C. Li, K. Ting, C. Soo and Z. Zheng, Current development of biodegradable polymeric materials for biomedical applications, *Drug Des., Dev. Ther.*, 2018, **12**, 3117–3145.
11 M. G. Patino, M. E. Neiders, S. Andreana, B. Noble and R. E. Cohen, Collagen: an overview, *Implant Dent.*, 2002, **11**(3), 280–285.
12 S. S. Mathew-Steiner, S. Roy and C. K. Sen, Collagen in wound healing, *Bioengineering*, 2021, **8**(5), 63.
13 F. Copes, N. Pien, S. Van Vlierberghe, F. Boccafoschi and D. Mantovani, Collagen-based tissue engineering strategies for vascular medicine, *Front. Bioeng. Biotechnol.*, 2019, **7**, 166.
14 R. Parenteau-Bareil, R. Gauvin and F. Berthod, Collagen-based biomaterials for tissue engineering applications, *Materials*, 2010, **3**(3), 1863–1887.
15 C. H. Lee, A. Singla and Y. Lee, Biomedical applications of collagen, *Int. J. Pharm.*, 2001, **221**(1–2), 1–22.
16 A. A. El-Sawah, N. E. A. El-Naggar, H. E. Eldegla and H. M. Soliman, Green synthesis of collagen nanoparticles by *Streptomyces xinghaiensis* NEAA-1, statistical optimization, characterization, and evaluation of their anticancer potential, *Sci. Rep.*, 2024, **14**(1), 3283.
17 A. A. El-Sawah, N. E. A. El-Naggar, H. E. Eldegla and H. M. Soliman, Bionanofactory for green synthesis of collagen nanoparticles, characterization, optimization, in-vitro and in-vivo anticancer activities, *Sci. Rep.*, 2024, **14**(1), 6328.
18 A. Arun, P. Malrautu, A. Laha, H. Luo and S. Ramakrishna, Collagen nanoparticles in drug delivery systems and tissue engineering, *Appl. Sci.*, 2021, **11**(23), 11369.
19 P. Rathore, I. Arora, S. Rastogi, M. Akhtar, S. Singh and M. Samim, Collagen nanoparticle-mediated brain silymarin delivery: an approach for treating cerebral ischemia and reperfusion-induced brain injury, *Front. Neurosci.*, 2020, **14**, 538404.
20 E. I. Alarcon, K. Udekwu, M. Skog, N. L. Pacioni, K. G. Stamplecoskie, M. González-Béjar, *et al.*, The biocompatibility and antibacterial properties of collagen-stabilized, photochemically prepared silver nanoparticles, *Biomaterials*, 2012, **33**(19), 4947–4956.
21 V. S. Cardoso, P. V. Quelemes, A. Amorin, F. L. Primo, G. G. Gobo, A. C. Tedesco, *et al.*, Collagen-based silver nanoparticles for biological applications: synthesis and characterization, *J. Nanobiotechnol.*, 2014, **12**(1), 36.
22 C. You, Q. Li, X. Wang, P. Wu, J. K. Ho, R. Jin, *et al.*, Silver nanoparticle loaded collagen/chitosan scaffolds promote wound healing via regulating fibroblast migration and macrophage activation, *Sci. Rep.*, 2017, **7**(1), 10489.
23 R. Li, Z. Xu, Q. Jiang, Y. Zheng, Z. Chen and X. Chen, Characterization and biological evaluation of a novel silver nanoparticle-loaded collagen-chitosan dressing, *Regener. Biomater.*, 2020, **7**(4), 371–380.
24 A. Mandal, S. Sekar, N. Chandrasekaran, A. Mukherjee and T. P. Sastry, Synthesis, characterization and evaluation of collagen scaffolds crosslinked with aminosilane functionalized silver nanoparticles: in vitro and in vivo studies, *J. Mater. Chem. B*, 2015, **3**(15), 3032–3043.
25 N. Duraipandy, R. Lakra, K. V. Srivatsan, U. Ramamoorthy, P. S. Korrapati and M. S. Kiran, Plumbagin caged silver nanoparticle stabilized collagen scaffold for wound dressing, *J. Mater. Chem. B*, 2015, **3**(7), 1415–1425.
26 C. Deepa, G. Suresh, P. Devagi, A. Kowsalya, K. Kavitha and B. Ramesh, Evaluation of the antibacterial activity of silver nanoparticles, doxycycline, collagen and their amalgamation–an in vitro study, *Mater. Today Proc.*, 2021, **43**, 3050–3053.
27 K. Ye, Y. Ke, N. Keshava, J. Shanks, J. A. Kapp, R. R. Tekmal, *et al.*, Opium alkaloid noscapine is an antitumor agent that arrests metaphase and induces apoptosis in dividing cells, *Proc. Natl. Acad. Sci. U. S. A.*, 1998, **95**(4), 1601–1606.
28 H. Chugh, P. Kumar, N. Kumar, R. K. Gaur, G. Dhawan and R. Chandra, Ex vivo binding studies of the anti-cancer drug noscapine with human hemoglobin: a spectroscopic and molecular docking study, *New J. Chem.*, 2021, **45**(3), 1525–1534.
29 H. Chugh, P. Kumar, V. Tomar, N. Kaur, D. Sood and R. Chandra, Interaction of noscapine with human serum

albumin (HSA): a spectroscopic and molecular modelling approach, *J. Photochem. Photobiol., A*, 2019, **372**, 168–176.

30 A. Bagde, N. Patel, K. Patel, E. Nottingham and M. Singh, Sustained release dosage form of noscapine HCl using hot melt extrusion (HME) technique: formulation and pharmacokinetics, *Drug Delivery Transl. Res.*, 2021, **11**(3), 1156–1165.

31 S. Sebak, M. Mirzaei, M. Malhotra, A. Kulamarva and S. Prakash, Human serum albumin nanoparticles as an efficient noscapine drug delivery system for potential use in breast cancer: preparation and in vitro analysis, *Int. J. Nanomed.*, 2010, **5**, 525–532.

32 K. Yadav, D. Yadav, M. Yadav and S. Kumar, Noscapine loaded PLGA nanoparticles prepared using oil-in-water emulsion solvent evaporation method, *J. Nanopharmaceutics Drug Delivery*, 2016, **3**(1), 97–105.

33 S. S. Esnaashari and A. Amani, Optimization of noscapine-loaded mPEG-PLGA nanoparticles and release study: a response surface methodology approach, *J. Pharm. Innovation*, 2018, **13**(3), 237–246.

34 M. O. Abdalla, R. Aneja, D. Dean, V. Rangari, A. Russell, J. Jaynes, *et al.*, Synthesis and characterization of noscapine loaded magnetic polymeric nanoparticles, *J. Magn. Magn. Mater.*, 2010, **322**(2), 190–196.

35 K. Yadav, D. Yadav, S. Kumar, K. Narra, M. El-Sherbiny, R. H. Al-Serwi, *et al.*, Natural biodegradable and polymeric nanoparticles for the delivery of noscapine for cancer treatment, *Biomass Convers. Biorefin.*, 2024, **14**(21), 27609–27621.

36 K. Yadav, D. Yadav, M. Yadav and S. Kumar, Noscapine-loaded PLA nanoparticles: systematic study of effect of formulation and process variables on particle size, drug loading and entrapment efficiency, *Pharm. Nanotechnol.*, 2015, **3**(2), 134–147.

37 J. J. Otarola, M. A. Luna, M. Correa and P. G. Molina, Noscapine-loaded nanostructured lipid carriers as a potential topical delivery to bovine mastitis treatment, *ChemistrySelect*, 2020, **5**(20), 5922–5927.

38 J. Madan, N. Dhiman, S. Sardana, R. Aneja, R. Chandra and A. Katyal, Long-circulating poly(ethylene glycol)-grafted gelatin nanoparticles customized for intracellular delivery of noscapine: preparation, in-vitro characterization, structure elucidation, pharmacokinetics, and cytotoxicity analyses, *Anticancer Drugs*, 2011, **22**(6), 543–555.

39 A. M. E. Badawy, T. P. Luxton, R. G. Silva, K. G. Scheckel, M. T. Suidan and T. M. Tolaymat, Impact of environmental conditions (pH, ionic strength, and electrolyte type) on the surface charge and aggregation of silver nanoparticles suspensions, *Environ. Sci. Technol.*, 2010, **44**(4), 1260–1266.

40 P. Bélteky, A. Rónavári, N. Igaz, B. Szerencsés, I. Y. Tóth, I. Pfeiffer, *et al.*, Silver nanoparticles: aggregation behavior in biorelevant conditions and its impact on biological activity, *Int. J. Nanomed.*, 2019, **14**, 667–687.

41 S. Sewariya, H. Sehrawat, N. Mishra, M. B. Singh, P. Singh, S. Kukreti, *et al.*, Comparative assessment of 9-bromo noscapine ionic liquid and noscapine: synthesis, in-vitro studies plus computational & biophysical evaluation with human hemoglobin, *Int. J. Biol. Macromol.*, 2023, **247**, 125791.

42 I. Matai, A. Sachdev and P. Gopinath, Multicomponent 5-fluorouracil loaded PAMAM stabilized-silver nanocomposites synergistically induce apoptosis in human cancer cells, *Biomater. Sci.*, 2015, **3**(3), 457–468.

43 S. Shen, Y. Wu, Y. Liu and D. Wu, High drug-loading nanomedicines: progress, current status, and prospects, *Int. J. Nanomed.*, 2017, **12**, 4085–4109.

44 V. S. Cardoso, P. V. Quelemes, A. Amorin, F. L. Primo, G. G. Gobo, A. C. Tedesco, *et al.*, Collagen-based silver nanoparticles for biological applications: synthesis and characterization, *J. Nanobiotechnol.*, 2014, **12**(1), 36.

45 N. Soni, K. Jyoti, U. K. Jain, A. Katyal, R. Chandra and J. Madan, Noscapinoids bearing silver nanocrystals augmented drug delivery, cytotoxicity, apoptosis and cellular uptake in B16F1, mouse melanoma skin cancer cells, *Biomed. Pharmacother.*, 2017, **90**, 906–913.